JOURNAL OF PHYSICAL CHEMISTRY, 2025, Vol. 99, No. 1, c. 142–148

ELECTROCHEMISTRY. GENERATING AND STORING ENERGY FROM RENEWABLE SOURCES

STUDYING THE ELECTROCHEMICAL BEHAVIOR OF A SMOOTH GOLD ELECTRODE IN A SOLUTION OF BRIDGED 1,2,4-TRIOXALANE IN ACETONITRILE

M. V. Polyakov[a, *], M. D. Vedenyapina[a], A. M. Skundin[b], I. A. Yaryomenko[a], and P. S. Radulov[a]

[a] *Zelinsky Institute of Organic Chemistry of the Russian Academy of Sciences, Moscow, 119991 Russia*
[b] *Frumkin Institute of Physical Chemistry and Electrochemistry of the Russian Academy of Sciences, Moscow, 119071 Russia*
**e-mail: SatPolyak@yandex.ru*

Received March 27, 2024
Revised March 27, 2024
Accepted April 09, 2024

Abstract. The behavior of a smooth gold electrode in the medium of bridged 1,2,4-trioxalane in acetonitrile is studied by cyclic voltammetry and gravimetry methods. It is found that during the cathodic process, the reduction of the peroxide bond in the bridged 1,2,4-trioxalane molecule takes place at the electrode surface followed by the formation of a diketone moiety. During anodic oxidation, the formation of colloidal gold particles is detected.

Keywords: *cyclic voltammetry, cathodic reduction, anodic oxidation, 1,2,4-trioxalane, gold*

DOI: 10.31857/S00444537250115e3

Organic peroxides have a wide range of biological activities such as fungicidal [1–4], anthelmintic [5–8], anticancer [1, 9–13], antimalarial [10, 14–16], and antiprotozoarian [5, 11, 17, 18]; these compounds are also still interesting as initiators of radical polymerization for industrial processes [19–21] — for these reasons, it is still relevant to develop various methods of their synthesis and analysis [22–25].

Using electrochemical analysis methods, one can determine the potential redox power of compounds, in particular organic peroxides. The cyclic voltammetry method is one of the most common methods [26–28]. Moreover, such studies were undertaken both to establish a correlation between biological activity and redox power of compounds [10, 29] and to determine the ongoing processes of oxidation and reduction of peroxides on electrodes [28, 30–32] created from certain materials, in various organic and aqueous media.

The works [28, 30, 31, 33, 34] studied the electrochemical behavior of organic peroxides in the medium of organic solvents using a glassy carbon electrode as a working electrode. One can also find a number of works in which the redox properties of organic peroxides were studied in the aqueous medium, but in this case the working electrode was gold or platinum [32, 35–38]. Thus, we found it extremely interesting to study such compounds in non-aqueous media on noble metal electrodes.

Ethyl 2-(4-chlorobenzyl)-1,5-dimethyl-6,7,8-trioxabicyclo[3.2.1]octane-2-carboxylate (**3**) was prepared according to the method [3] in two stages from the ethyl ester of 2-(4-chlorobenzyl)-3-oxobutanoate (**1**) (Scheme 1).

The product of the reduction reaction of 1,2,4-trioxolane (ozonide) **3** was the initial 1,5-diketone **2**, which was isolated individually using column chromatography. Compounds **2** and **3** were characterized by NMR spectroscopy.

The ^{1}H and ^{13}C NMR spectra were recorded on a Bruker AM-300 unit with the operating frequency 300 (^{1}H) or 75 (^{13}C) MHz. The internal standard was $CHCl_3$. ^{1}H NMR chemical shifts are given relative to the residual signal of the solvent (CDCl3) of 7.27 ppm for ^{1}H nuclei and 77.0 ppm for ^{13}C nuclei.

Chromatography of the products was performed on silica gel (0.060–0.200 mm, 60°, CAS 7631-86-9). Dichloromethane, acetonitrile, petroleum ether (PE). (40 : 70), ethyl acetate (EA), methyl vinyl ketone, H_2O_2 (35% aqueous solution), $MgSO_4$, $NaHCO_3$, NaI, $CeCl_3 \cdot 7H_2O$, $BF_3 \cdot Et_2O$, and $Na_2S_2O_3$ were purchased from Acros. A solution of H_2O_2 in Et_2O (6.0 m) was obtained by extraction of Et_2O (5–100 mL) from a 35% aqueous solution (100 mL) followed by drying over $MgSO_4$ and removal of a portion of Et_2O in the

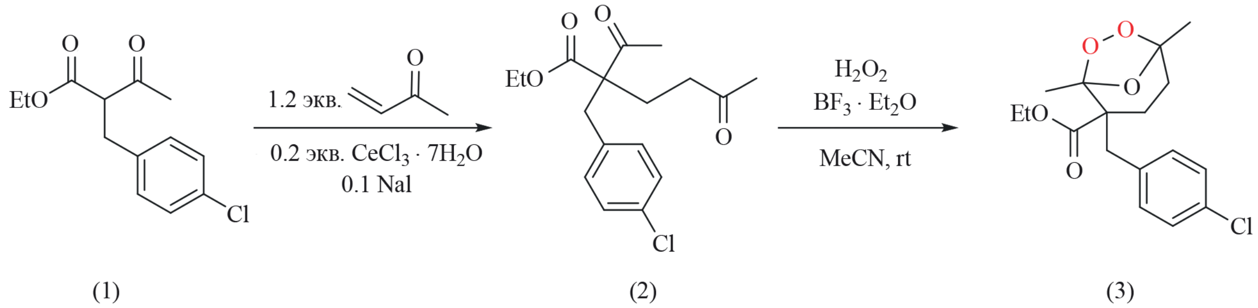

Scheme 1. Preparation of the test substrate **3**.

vacuum of a water jet pump at 20–25°C. The ethyl ester of 2-acetyl-2-(4-chlorobenzyl)-5-oxahexanoic acid (**2**) was obtained according to the technique [3]. The spectral characteristics of compounds 2,3 corresponded to those described earlier [3].

Ethyl ester of 2-acetyl-2-(4-chlorobenzyl)-5-oxahexanoic acid, 2

Light yellow oil. 85% yield.

^{1}H NMR spectrum (300.13 MHz, δ, ppm, J/Hz, CDCl$_3$): 1.26 (t, 3H, J = 7.1 Hz), 2.02 – 2.36 (m, 8H), 2.38 – 2,65 (m, 2H), 3.05 – 3.23 (dd, 2H, J=14.2 Hz), 4.13 – 4.23 (m, 2H), 7.00 (d, 2H, J = 8.2 Hz), 7.22 (d, 2H, J = 8.2 Hz).

^{13}C NMR spectrum (75.48 MHz, δ, ppm, J/Hz, CDCl$_3$): 14.0, 25.6, 27.6, 30.1, 37.7, 38.2, 61.7, 63.9, 128.6, 129.2, 130.2, 131.3, 171.6, 205.2, 206.8.

Ethyl 2-(4-chlorobenzyl)-1,5-dimethyl-6,7,8-trioxabicyclo[3.2.1]octane-2-carboxylate, 3

White crystals. 90% yield. R$_f$ = 0.46 (TLC, PE : EA, 5 : 1).

^{1}H NMR spectrum (300.13 MHz, δ, ppm, J/Hz, CDCl$_3$): 1.22 (t, J = 7.2 Hz, 2.5H), 1.26 (t, J = 7.2 Hz, 0.5H), 1.48 (s, 2.5H), 1.55 (s, 0.5H), 1.59 – 2.11 (m, 4.2H), 1.66 (s, 0.5H), 1.79 (s, 2.5H), 2.59 (d, J = 12.9 Hz, 1H), 3.00 (d, J = 12.9 Hz, 0.2H), 3.30 (d, J = 12.9 Hz, 0.2H), 4.14 (q, J = 7.2 Hz, 0.4H), 4.19 (q, J = 7.2 Hz, 1.6H), 7.00 (d, J = 8.8 Hz, 1.6H), 7.04 (d, J = 8.8 Hz, 0.4H), 7.21 (d, J = 8.8 Hz, 1.6H), 7.22 (d, J = 8.8 Hz, 0.4H).

^{13}C NMR spectrum (75.48 MHz, δ, ppm, J/Hz, CDCl$_3$): 14.2, 18.7, 19.0, 20.6, 20.8, 21.7, 25.7, 31.1, 32.8, 36.9, 40.3, 54.1, 54.4, 61.2, 61.4, 109.2, 109.8, 111.0, 111.2, 128.5, 128.6, 131.3, 131.4, 132.9, 134.6, 172.3, 172.4.

In this work, 2-(4-chlorobenzyl)-1,5-dimethyl-6,7,8-trioxabicyclo[3.2.1]octane-2-carboxylate **3** was studied for its electrochemical behavior on gold electrode in acetonitrile medium by CVA (cyclic voltammetry) method, also the cathodic reduction product on the gold electrode was determined and the corrosion kinetics of gold during anodic oxidation in the presence of compound **3** was studied.

EXPERIMENTAL PART

CVA Study

Cyclic voltammetry was recorded using an IPC-Pro MF potentiostat controlled by a personal computer. The studies were carried out in a three-electrode cell at a temperature of 293 K in the region of potentials E from –2800 to 2300 mV. The potential sweep rate was varied in the range from 100 to 500 mV/s. A gold wire with a diameter of 0.3 mm soldered into glass and immersed in the electrolyte solution for 5 mm was used as a working electrode; a platinum wire of the same size served as an auxiliary electrode. To specify the processes occurring in the anodic region, a gold disk electrode with a working area of 50.26 mm^2 was used. The reference electrode was a silver chloride electrode with a double membrane (Ag|AgCl|KCl (3.5 mol l^{-1})). Prior to the experiment, the platinum and gold electrode were etched in aqua regia and subjected to cathodic polarization in 0.1 n sulfuric acid solution at j=20.9 mA/cm^2.

Working solutions were prepared using acetonitrile (MeCN) prehydrated over P$_2$O$_5$. A 0.05 M solution of tetrabutylammonium hexafluorophosphate (Bu$_4$NPF$_6$, TBAFP) in acetonitrile was used as a background electrolyte, the concentration of the studied compound **3** was 0.05 M in the case of the study on a smooth gold electrode in the cathodic region, and the concentration of 1 was 0.03 M in the case of scanning on a gold disk electrode in the anodic region.

Electrolysis Using Au as a Cathode

Electrolysis was carried out in a two-electrode cell without separation of anode and cathode spaces for the current I = 1 mA using gold wire (d = 0.3 mm) as cathode and platinum wire (d = 0. 3 mm) as anode in 5 mL of a solution of compound **3** (the

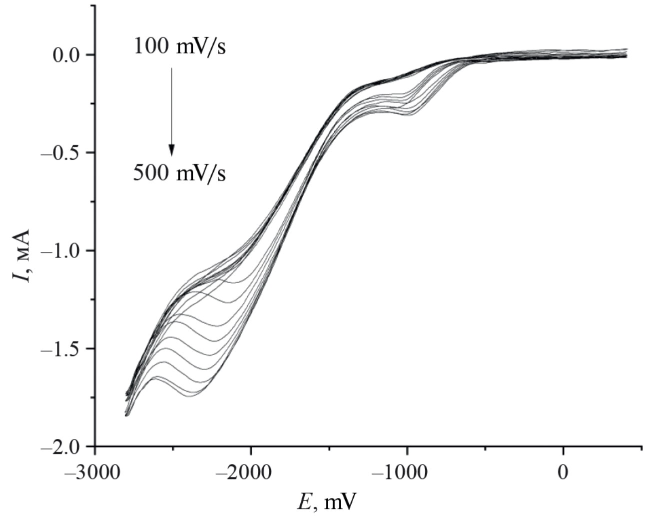

Fig. 1. CVA **3** in the cathodic region on the Au electrode, ν = 100, 150, 200, 250, 300, 350, 400, 450, 500 mV/s.

concentration 0.075 mol l^{-1}) in acetonitrile, using tetrabutylammonium tetrafluoroborate (Bu_4NBF_4, TBAFB) with a concentration of 0.05 mol l^{-1} for conductivity.

Electrolysis Using Au as an Anode

Corrosion of gold anode during electrolysis was studied in a two-electrode cell without separation of anode and cathode spaces for the current $I = 5$ mA. A platinum wire ($d = 0.3$ mm) was used as the cathode, the gold anode was also a wire ($d = 0.3$ mm), and both electrodes were immersed 11-12 mm into the solution. The concentration of compound **3** used was 0.05 M in the solution of Bu_4NPF_6 (0.05 M) in acetonitrile, and the volume of the working solution was 5 mL. In order to estimate the loss (or gain) of the electrode mass at certain time intervals, the electrodes were weighed on ABJ220-4NM electronic analytical scales (Kern, USA) ($d = 0.0001$ g).

The presence of gold particles in the solution was determined by X-ray fluorescence spectrometry with graduation according to the method of fundamental parameters on an ARL PFX-101 X-ray fluorescence spectrometer (Thermo ARL, Switzerland).

DISCUSSION OF RESULTS

When the gold electrode was immersed in the solution under study, a steady-state potential of 0.4 V was set relative to the silver chloride reference electrode, and then CVA of the solution of compound **3** with the concentration 0.05 M was recorded.

Figure 1 shows CVA recorded for the gold electrode in solution **3** in the potential range E from 400 mV to −2800 mV, for different potential scanning frequences ν from 100 to 500 mV/s. Two irreversible peaks are observed on CVA, viz. the first one implicitly expressed in the potential interval from −800 to −1150 mV, and the second one in the potential interval from −1500 to −2600 mV.

Figure 2 shows the linear dependencies $I_{p,c} - \nu^{0.5}$ passing through the coordinate origin or close to it, which indicates that the recovery in both cathodic processes in the studied potential intervals is limited by the stage of diffusive supply of the substrate to the electrode surface [39, 40]; therefore, the equation is applicable in this case

$$I_{p,c} = 0.496 S\alpha^{0.5} n_{\alpha}^{0.5} nFc_0 \left(\frac{FD}{RT}\right)^{0.5} \nu^{0.5},$$

where S is the surface area of the working electrode immersed in the solution, cm^2, c_0 is the concentration of the test substance in the cell, mol/cm^3, F is the Faraday number, C/mol, R is the universal gas constant, J/(K mol), T is the absolute temperature value during the experiment, K, D is the diffusion coefficient, cm^2/s, α is the electron transfer coefficient, $n\alpha$ is the number of electrons participating in the limiting stage of charge transfer, n is the total number of electrons carried by the diffusing particle. Generally, $n\alpha = 1$.

The values αn_a were calculated for cathodic processes. The values αn_a were calculated by the formula

$$\alpha n_a = \frac{1.857RT}{F\Delta E_{p/2}}, \tag{2}$$

where R is the universal gas constant, J/(K mol), T is the absolute temperature value during the experiment, K, F is the Faraday number, C/mol, and $E_{p/2}$ is the potential value for $0.5I_{p,c,}$ V. For each potential sweep rate for each cathodic peak, the arithmetic mean values of αn_a were then found.

According to the calculations based on the obtained data of Fig. 2, $\alpha_1 n_\alpha = 0.5$ for the first cathodic peak and $\alpha_2 n_\alpha = 0.32$ for the second cathodic peak. Both of these values are within the range $0 < \alpha < 0.5$, so it can be assumed that $n_a = 1$.

Reproducible CVA were obtained by recording CVA on the gold disk electrode with a radius of 4 mm in the potential range E from 400 to 2300 mV. The anodic peak was recorded in the potential range from 1200 to 2300 mV. As the potential sweep rate increased, the potential value of the maximum current shifted to

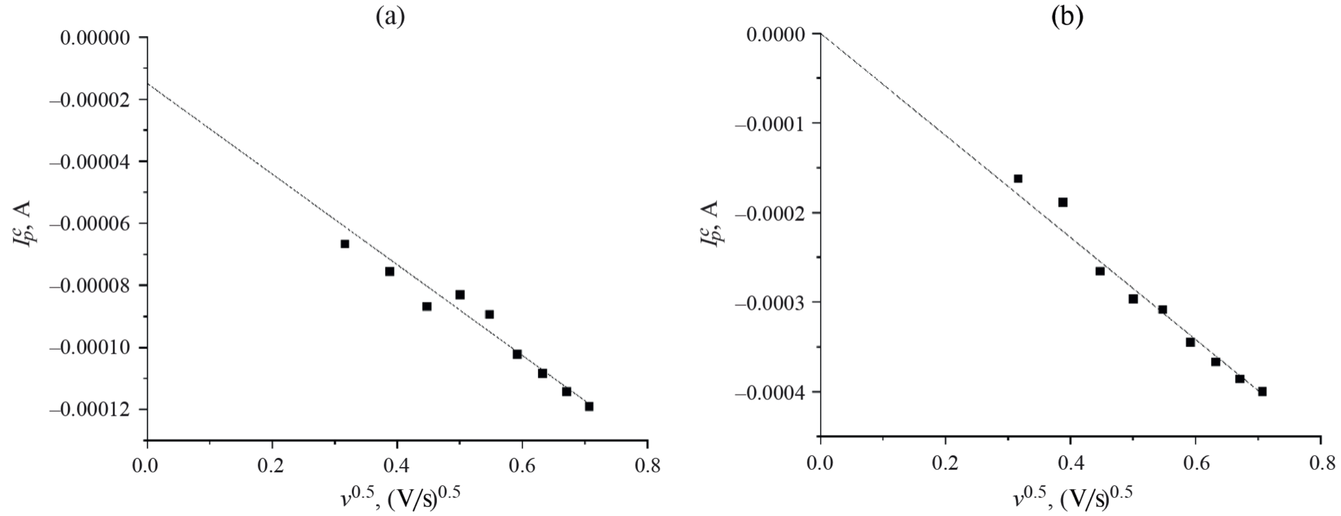

Fig. 2. Dependences $I_p^c - \nu^{0.5}$ for the first (a) and second (b) cathode peaks of CVA.

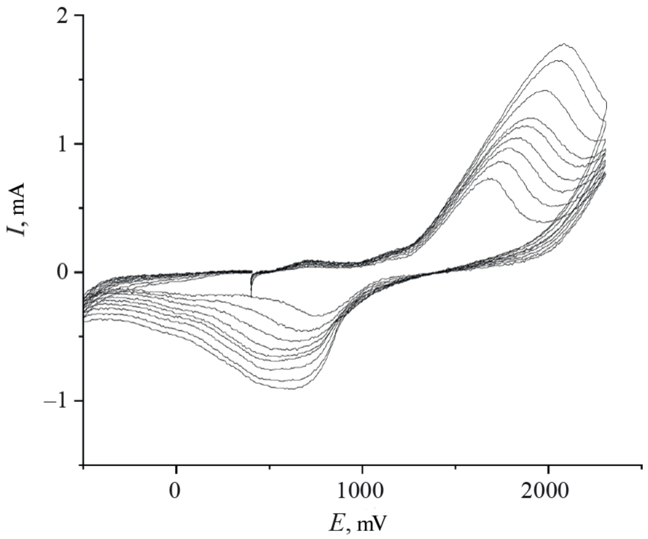

Fig. 3. CVA **3** in the anodic region on the Au electrode, ν = 100, 150, 200, 250, 300, 350, 400, 450, 500 mV/s.

the deeper anodic region. A quasi-reversible recovery peak was also observed in the cathodic branch of the CVA sweep (Fig. 3).

Using equation (1), the substrate diffusion coefficients were calculated, given the already found value of the coefficient α. The surface area S was 4.78×10^{-6} m^2 given that the diameter of the working electrode was 0.3 mm and the immersion in the solution was 5 mm. From formula (1), taking into account the slopes of the straight lines of Fig. 4, the diffusion coefficients D were calculated, assuming that one electron $n = 1$ is transferred in each of the processes. The slopes of the straight lines are respectively $\frac{dI}{dv^{0,5}} = -1.33 \times 10^{-4}$ As$^{1/2}$/V$^{1/2}$ for the first cathodic peak and $\frac{dI}{dv^{0,5}} = -5.695 \times 10^{-4}$ As$^{1/2}$/V$^{1/2}$ for the second cathodic peak, and the calculated diffusion coefficients are $D_{\text{c},1} = 6.85 \times 10^{-8}$ cm^2/s, $D_{\text{c},2} = 1.95 \times 10^{-6}$ cm^2/s.

Note the difference between the diffusion coefficients, which differ from each other by one and a half orders of magnitude, with the largest value of D calculated for the second process. A similar difference in diffusion coefficients was observed while studying the electrochemical behavior of 1,2,4,5-tetraoxane in acetonitrile medium [41]. Apparently, the radical formed by the first cathodic process is more mobile than the initial cyclic peroxide, which is the reason for the difference between the diffusion coefficients $D_{\text{c},1}$ and $D_{\text{c},2}$.

The dependence of $I_{p,a}$ on the square root of the potential scan rate $\nu^{0.5}$ is a straight line passing through the coordinate origin (Fig. 4), which indicates that the anodic process in the studied potential range is limited by the stage of diffusive substrate supply to the electrode surface. Therefore, Eq. (1) is applicable in this case, as well as for the processes occurring in the cathodic region of CVA.

The calculation carried out by Eq. (2), using the data obtained from Fig. 4, allowed us to calculate the value $\alpha_1 n\alpha$ for the anodic process. This value equaling 0.28 lies in $0 < \alpha < 0.5$, so we can consider that $n_\alpha = 1$.

Using Eq. (1), we calculated the substrate diffusion coefficient D taking into account the surface area S equaling 4.94×10^{-5} m^2 for the disk Au electrode,

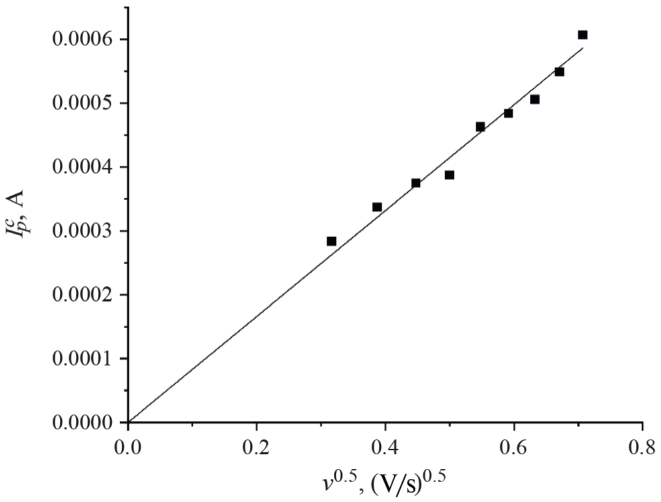

Fig. 4. $I_{p,a}$ depending on $\nu^{0,5}$.

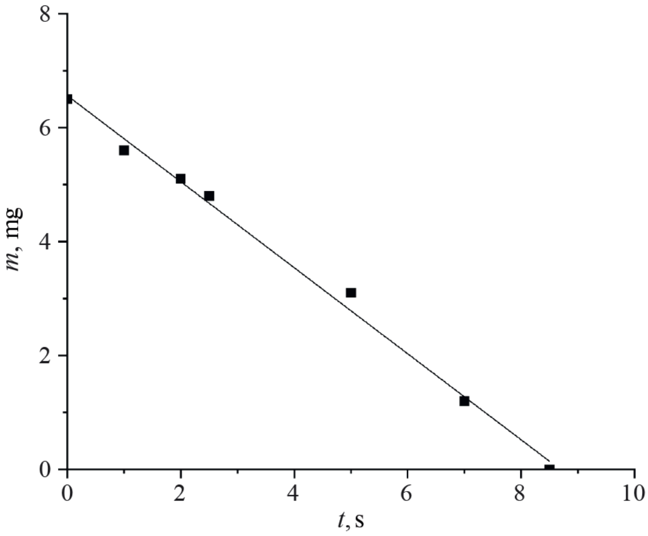

Fig. 5. Change of the gold anode mass, for I = 5 мA, in the MeCN solution, the concentration of compound **3** was 0.05 M.

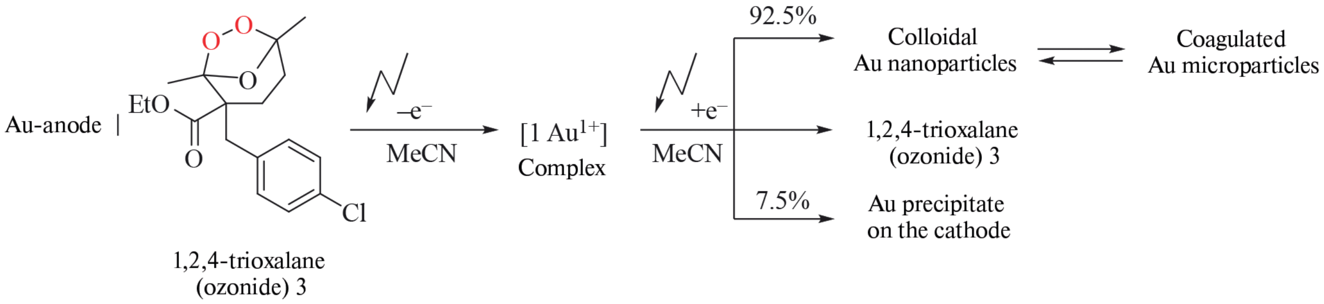

Scheme 2. Electrochemical corrosion of gold in the presence of compound 3 in the acetonitrile medium.

and the slope of the straight line (data of Fig. 4) being $\frac{dI}{dv^{0,5}} = 8.29 \times 10^{-4}$ $As^{1/2}/V^{1/2}$. The value of the diffusion coefficient for the anodic process is $D_a = 1.25 \times 10^{-7}$ cm^2/s.

In order to study the oxidation products, a gravimetric experiment was carried out, where a smooth gold electrode was used as the anode and a platinum electrode was used as the cathode (Fig. 5). The mass of the platinum cathode increased by 0.5 mg throughout the experiment while the mass of gold dissolved from the anode was 6.5 mg. During electrolysis with the platinum cathode, a linear dependence of gold dissolution on the time of the experiment is observed.

We have proposed the following mechanism of the anodic corrosion process of the gold electrode (Scheme 2)

During electrolysis with a gold electrode used as a cathode with I = 1 mA, the formation of 1,5-diketone **2**, which was the starting compound for the synthesis of bridging 1,2,4-trioxalane **3**, was recorded (Scheme 3). Note that the yield of product **2** during 45 hours of electrolysis was 39 %. When attempting to hold the reaction at higher current values (I = 5 mA, I = 10 mA), product **2** was detected only in trace amounts by NMR spectroscopy. Apparently, compound **2** is not formed at higher current values.

CONCLUSIONS

When studying the electrochemical behavior of a smooth gold electrode in a solution of bridging 1,2,4-trioxalane in acetonitrile, we found that the reduction of the peroxide bond occurs in the cathodic region with the transfer of two electrons followed by the breaking of the cycle in compound **3**, with a 1,5-diketone fragment formed as a result. The gravimetric method showed that corrosion of the gold electrode occurs in the anode space with gold nanoparticles formed, and the transfer of gold particles to the cathode is practically not observed.

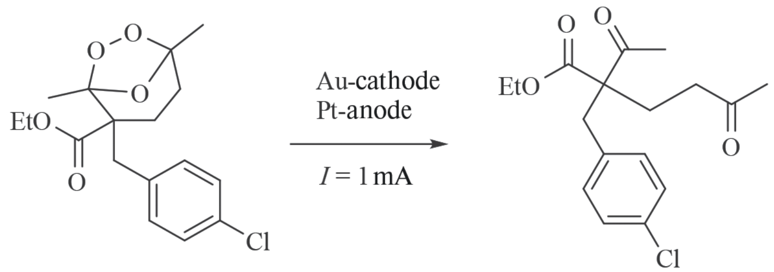

(3) (2)

Scheme 3. Cathodic reduction reaction of compound **3**.

FUNDING

The work was carried out within the framework of the State Assignment of Institute of Organic Chemistry of the Russian Academy of Sciences (topic no. FFZZ-2022-03).

ETHICS DECLARATIONS

This work does not contain any studies involving human and animal subjects.

CONFLICT OF INTEREST

The authors of this work declare that they have no conflicts of interest.

REFERENCES

1. *Ann Casteel D.//* Nat. Prod. Rep. 1999. Vol. 16. No. 1. P. 55. DOI: 10.1039/A705725C
2. *Phillipson D. W., Rinehart, K. L. Jr.//* J. Am. Chem. Soc. 1983. Vol. 105. No. 26. Pp. 7735–7736. DOI: 10.1039/A705725C
3. *Yaremenko I. A., Radulov P. S., Belyakova Y. Y. et al.* // Chem. Europ. J. 2020. Vol. 26. No. 21. P. 4734. DOI: 10.1002/chem.201904555
4. *Yaremenko I. A., Syromyatnikov M. Y., Radulov P. S. et al.* // Molecules. 2020. Vol. 25. No. 8. P. 1954. DOI: 10.3390/molecules25081954
5. *Panic G., Duthaler U., Speich B., Keiser J.* // Int. J. Parasitol. Drugs Drug. Resist. 2014. Vol. 4. No. 3. P. 185. DOI: 10.1016/j.ijpddr.2014.07.002
6. *Vil' V. A., Yaremenko I. A., Ilovaisky A. I., Terent'ev A. O.* // Synthesis and Reactions. Molecules. 2017. Vol. 22. No. 11. P 1881. DOI: 10.3390/molecules22111881
7. *Kiuchi F., Itano Y., Uchiyama N. et al.* // J. Am. Pharm. Assoc. 2002. Vol. 65. No. 4. P. 509. DOI: 10.1021/np010445g
8. *Wenzel D.G., Smith C.M.* // J. Am. Pharm. Assoc. Am. Pharm. Assoc. 1958. Vol. 47. No. 11. P. 792. DOI: 10.1002/jps.3030471109
9. *Herrmann L., Yaremenko I. A., Çapcı A. et al.* // ChemMedChem. 2022. Vol. 17. No. 9. DOI: 10.1002/cmdc.202200005
10. *Coghi P. Yaremenko I. A., Prommana P. et al.* // ChemMedChem. 2022. Vol. 17. No. 20. DOI: 10.1002/cmdc.202200328
11. *Slade D., Galal A. M., Gul W. et al.* // Bioorg. Med. Chem. 2009. Vol. 17. No. 23. P. 7949. DOI: 10.1016/j.bmc.2009.10.019
12. *Yaremenko I. A., Coghi P., Prommana P. et al.* // ChemMedChem 2020. Vol. 15. No. 13. Pp. 1118–1127. DOI: 10.1002/cmdc.202000042
13. *Yaremenko I. A., Syroeshkin M. A., Levitsky D. et al.* // Med. Chem. Res. 2017. Vol. 26. No. 1. P. 170. DOI: 10.1007/s00044-016-1736-2
14. *Tiwari M. K., Chaudhary S.* // Med. Res. Rev. 2020. Vol. 40. No. 4. P. 1220. DOI: 10.1002/med.21657
15. *Uddin A., Chawla M., Irfan I. et al.* //. RSC Med. Chem. 2020. Vol. 12. No. 1. P. 24. DOI: 10.1039/d0md00244e
16. *Woodley C. M., Amado P. S. M., Cristiano M. L. S., O'Neill, P. M.* // Med. Res. Rev. 2021. Vol. 41. No. 6. P. 3062. DOI: 10.1002/med.21849
17. *Otoguro K., Iwatsuki M., Ishiyama A. et al.* // Phytochem. 2011. Vol. 72. No. 16. P. 2024. DOI: 10.1016/j.phytochem.2011.07.015
18. *Perry T. L., Dickerson A., Khan A. A. et al.* // Tetrahedron. 2001. Vol. 57. No. 8. P. 1483. DOI: 10.1016/S0040-4020(00)01134-0
19. *Kumar M., Gehlot P. S., Parihar D. et al.* // Eur. Pol. J. 2021. Vol. 152. DOI: 10.1016/j.eurpolymj.2021.110448
20. *Lee M., Minoura Y.* // J. Chem. Soc., Faraday Trans. 1978. Vol. 74. No. 0. P. 1726. DOI: 10.1039/f19787401726

21. *Przybysz-Romatowska M., Haponiuk J., Formela K.* // Polymers. 2020. Vol. 12. No. 1. DOI: 10.3390/polym12010228
22. *Radulov P. S., Belyakova Y. Y., Demina A. A. et al.* // Russ. Chem. Bull. 2019. Vol. 68. No. 6. P. 1289. DOI: 10.1007/s11172-019-2555-7
23. *Matsumoto A., Maruoka K.* // Bull. Chem. Soc. Jpn. 2020. Vol. 94. No. 2. P. 513. DOI: 10.1246/bcsj.20200321
24. *Gemki M., Taspinar Ö., Adler A. et al.* // Org. Proc. Res. Dev. 2021. Vol. 25. No. 12. P. 2747. DOI: 10.1021/acs.oprd.1c00364
25. *Zdvizhkov, A., Terent'ev A., Radulov P. et al.* // Tetrahedron Lett. 2016. Vol. 57. No. 8. DOI: 10.1016/j.tetlet.2016.01.061
26. *Rountree E. S., McCarthy B. D., Eisenhart T. T., Dempsey J. L.* // Inorg. Chem. 2014. Vol. 53. No. 19. P. 9983.
27. *Savéant J.-M.* // Advances in Physical organic chemistry. 2000. Vol. 35. P. 117. DOI: 10.1016/s0065-3160(00)35013-4
28. *Magri D. C., Workentin M. S.* // Org. Biomol. Chem. 2008. Vol. 6. No. 18. P. 3354. DOI: 10.1039/b809356c
29. *Yaremenko I. A., Coghi P., Prommana P. et al.* // ChemMedChem. 2020. Vol. 15. No. 13. P. 1118. DOI: 10.1002/cmdc.202000042
30. *Magri D. C., Workentin M. S.* // Molecules. 2014. Vol. 19. No. 8. P. 11999. DOI: 10.3390/molecules190811999
31. *Magri D. C., Workentin M. S.* // Chemistry. 2008. Vol. 14. No. 6. P. 1698. DOI: 10.1002/chem.200701740
32. *Vedenyapina M. D., Simakova A. P., Platonov M. M. et al.* // Russ. J. Phys. Chem. DOI: 10.1134/S0036024413030333
33. *Magri D. C., Donkers R. L., Workentin M. S.* // J. Photochem. Photobiol., A. 2001. Vol. 138. No. 1. P. 29. DOI: 10.1016/S1010-6030(00)00386-5
34. *Stringle D. L., Magri D. C., Workentin M. S.* // Chemistry. 2010. Vol. 16. No. 1. P. 178. DOI: 10.1002/chem.200902023
35. *Vedenyapina M. D., Skundin A. M., Vil' V. A. et al.* // Russ. J. Phys. Chem. DOI: 10.1134/S0036024420040238
36. *Vedenyapina M. D., Skundin A. M., Vil' V. A. et al.* // Russ. J. Phys. Chem. DOI: 10.1134/S0036024421010313
37. *Vedenyapina M. D., Vil' V. A., Terent'ev A.O., Vedenyapin A. A.* // Russ. Chem. Bull. 2017. Vol. 66. No. 11. C. 2044.
38. *Polyakov M. V., Vedenyapina M. D., Skundin A. M. et al.* // Russ. J. Phys. Chem. Vol. 97. P. 1438. DOI: 10.1134/S0036024423070221
39. *Batchelor-McAuley C., Compton R. G.* // J. Electroan. Chem. 2012. Vol. 669. P. 73. DOI: 10.1016/j.jelechem.2012.01.016
40. *Salah N., Lanez T.* // Int. Lett. Chem. Phys. Astron. 2013. Vol. 4. P. 37.
41. *Polyakov M.V., Vedenyapina M.D., Skundin A.M. et al.* // Russ Chem Bull. 2024. Vol. 74. No. 4. P. 863.